

# Energy-Aware Hierarchical Cell Configuration: from Deployment to Operation

Kyuhoo Son, Eunsung Oh and Bhaskar Krishnamachari

Department of Electrical Engineering, Viterbi School of Engineering

University of Southern California, Los Angeles, CA, 90089

Email: {kyuhoo.son, eunsung.oh and bkrishna}@usc.edu

## Abstract

In this paper, we develop an energy-aware hierarchical cell configuration framework that encompasses both deployment and operation in downlink cellular networks. Specifically, we first formulate a general problem pertaining to total energy consumption minimization while satisfying the requirement of area spectral efficiency (ASE), and then decompose it into deployment problem at peak time and operation problem at off-peak time. For the deployment problem, we start from an observation about various topologies including the real deployment of BSs that there is a strong correlation between the area covered by an additional micro BS and the increment of ASE. Under such an assumption, we prove the submodularity of the ASE function with respect to micro BS deployment. We also show that the ASE increment achieved by an optimal placement with the same number of micro BSs as the greedy algorithm cannot be more than a factor of  $e/(e-1)$  from the ASE increment achieved by the greedy algorithm. Although the greedy algorithm can be also applied as an offline centralized solution for the operation problem, we further propose online distributed algorithms with low complexity and signaling overhead using Lagrangian relaxation to have more practical solutions. Extensive simulations based on the acquired real BS topologies and traffic profiles show that the proposed deployment and operation algorithms can dramatically reduce the total energy consumption, which in turn will boost the revenue of wireless network operators.

## Index Terms

Energy-aware, green cellular networks, hierarchical cell configuration, deployment, operation, area spectral efficiency;

## I. INTRODUCTION

Pushed by the explosive traffic demand from bandwidth-hungry multimedia and Internet-related services in broadband cellular networks, communication engineers seek to maximally exploit the spectral resources in all available dimensions. Hierarchical cell structure (HCS) [1], [2] where small cells such as micro, pico and femto are used as a way of incrementally increasing capacity and coverage beyond the initial deployment of macro cells, has

recently emerged as a promising solution, and is also being considered in many standardization bodies such as IEEE 802.16m (WiMax2) and 3GPP-LTE. Incrementally deploying micro base stations (BSs) is simpler than building out complex cell towers and macro BSs, and it can also reduce both capital (e.g., hardware) and operating (e.g., electricity, backhaul and site lease) expenditures [1], which is especially attracted to wireless network operators.

In the meantime, there is a growing consensus on the need to develop more energy-efficient networks (referred to as green networking) with the depletion of non-renewable resources and constraints on CO<sub>2</sub> emissions. From the perspective of wireless network operators, reducing electrical energy consumption is not only a matter of being green and responsible, but also an economically important issue. It is estimated that the operators are spending more than 10 billion dollars as of now globally with 60-80% of the total energy consumption being contributed by BS infrastructure [3]. Since BSs are being deployed by the operator targeting peak traffic usage, they are under-utilized most of the time. However, even when a site is experiencing little or no activity, the BS consumes more than 90% of its peak energy (e.g., a typical BS consumes between 800-1500W and has an transmission power of 20-40W). Beyond turning off only radio transceivers, dynamic approaches [4], [5] that allow the system to entirely switch off some under-utilized BSs and transfer the corresponding load to neighboring cells during low traffic period can substantially reduce the amount of wasted energy.

#### A. *Our Objective and Contributions*

In order to unburden wireless network operators from huge capital and operating expenditures (CAPEX & OPEX) while meeting the quality of service requirement, this paper focuses on providing theoretical implications and practical solutions for the following two key questions each of which is related to HCS deployment and operation:

- Where and how many micro BSs need to be deployed?
- How to operate (i.e., switching on-off) macro and micro BSs for energy conservation during off-peak times?

First, in the deployment problem, we try to find a minimal deployment of micro BSs while satisfying the requirement of area spectral efficiency (ASE). We make an observation from various topologies that there is a monotone relationship between coverage and ASE increment. Under such an assumption, we prove the submodularity of the ASE function with respect to micro BS deployment and propose a greedy algorithm, which has a nice feature of constant-factor approximation. Extensive simulations demonstrate that deploying micro BSs rather than conventional macro BSs can bring about 75-80% reduction of total operational energy consumption.

Second, in the operation problem, we want to minimize energy consumption through dynamic BS operation. Although the above greedy deployment algorithm can be also applied as a centralized offline solution for this problem, we further propose two distributed online algorithms using Lagrangian relaxation to have more practical solutions. Simulations based on traffic profiles from a real cellular system data trace show that the proposed

algorithms not only can achieve the near performance of the centralized algorithm but also can significantly reduce the energy consumption by 80-95%, compared to the case without the dynamic BS operation.

## B. Related Work

Most of the research on HCS has focused on resource allocation, e.g., spectrum allocation [6]–[8], power control [9], [10]; however, there has been relatively little work dealing with BS deployment in HCS. The studies in [11], [12] showed the benefit of HCS deployment in hexagonal networks only by simulations. In the non-HCS setting (i.e., only one type of BS), several BS deployment problems [13], [14] have been theoretically investigated. Stamatelos *et al.* [13] showed that an algorithm minimizing the overlapped coverage (i.e., the co-channel interference area) can maximize spectral efficiency in omni-antenna case. Srinivas *et al.* [14] proposed an algorithm which jointly considers both BS deployment and UE assignment in backbone base mobile ad-hoc networks for throughput optimization. Our work differs from the previous works in that: (i) we present an analytical framework for optimal BS deployment in HCS with the different types of BSs, and (ii) run extensive simulations based on BS topologies and traffic profiles acquired from real cellular networks.

Green networking has recently received significant attention. In [3]–[5], [15], [16], the authors investigated dynamic BS operation (i.e., switching-on/off BSs depending on the traffic profile) to save energy consumptions. In addition, the concept of BS sharing, where different operators pool their BSs together to further conserve energy, was introduced in [3], [17]. However, most of the previous works [3], [4], [15], [17] attempted to see how much energy saving can be achieved rather than developing algorithms that can be implemented in practice. Although several preliminary BS switching algorithms can be found in [5], [15], [16], they cannot capture the effect of the signal strength degradation when traffic loads are transferred from the switched-off BS to neighboring BSs. To reflect this effect, in this paper, (i) we consider a more sophisticated channel model based on SINR, and (ii) propose practical and distributed algorithms for the dynamic BS operation.

The remainder of this paper is organized as follows. In Section II, we formally describe our system model and general problem. In Section III and IV, we propose HCS deployment and operation algorithms, respectively. In Section V, we demonstrate the performance of the proposed algorithms under various topologies and scenarios including the real deployment of BSs and real traffic profiles. Finally, we conclude the paper in Section VI.

## II. SYSTEM DESCRIPTION AND PROBLEM DEFINITION

### A. System Description

1) *Network Model*: Consider a HCS broadband wireless network where the sets of macro and micro BSs, denoted by  $\mathcal{B}_M$  and  $\mathcal{B}_m$ , respectively, lie in the two-dimensional area  $\mathcal{A} \subset \mathbb{R}^2$ . Throughout the paper, subscript  $M$  is used for macro BSs, and  $m$  is for micro BSs. We focus on two types of BSs, but all discussions in this paper can be

readily extended to the general case where different types of BSs such as macro, micro, pico and even femto BSs are expected to coexist in a complex manner. Let us denote by  $b \in \mathcal{B} = \mathcal{B}_M \cup \mathcal{B}_m$  the index of BSs and by  $x_b$  the position of BS  $b$ , respectively. Our focus is on downlink communication as that is a primary usage mode for the mobile Internet, i.e., from BSs to user equipments (UEs). Although we focus on downlink communication, some aspects of our work can be applied to the uplink as well.

2) *Link Model*: The received signal strength from BS  $b$  to UE at location  $x$  can be expressed as  $E_b(x) = p_b \cdot g_b(x)$ , where  $p_b$  denotes the transmission power of BS  $b$ ,  $g_b(x)$  denotes the channel gain from BS  $b$  to location  $x$ , including path loss attenuation, shadowing and other factors if any. Note, however, that fast fading is not considered here because the time scale for measuring  $g_b(x)$  is assumed to be much larger. Accordingly, the signal to interference plus noise ratio (SINR) at location  $x$  can be written as:

$$\Gamma(x, \mathcal{B}) = \frac{E_{b(x, \mathcal{B})}(x)}{\sum_{b \in \mathcal{B}, b \neq b(x, \mathcal{B})} E_b(x) + \sigma^2}, \quad (1)$$

where  $\sigma^2$  is noise power and  $b(x, \mathcal{B})$  denotes the index of the BS at location  $x$  that provides the highest signal strength<sup>1</sup>, i.e.,  $b(x, \mathcal{B}) = \arg \max_{b \in \mathcal{B}} E_b(x)$ . Following Shannon's formula, spectral efficiency at location  $x$  is given by:

$$C(x, \mathcal{B}) = \log_2(1 + \Gamma(x, \mathcal{B})), \quad [\text{bit/sec/Hz}] \quad (2)$$

3) *Area Spectral Efficiency*: We adopt the area spectral efficiency (ASE) firstly introduced in [18] as our performance metric, which is defined as the summation of the spectral efficiency over the reference area  $\mathcal{A}$ :

$$S(\mathcal{A}, \mathcal{B}) \doteq \frac{\sum_{x \in \mathcal{X}} C(x, \mathcal{B}) \cdot Pr(x)}{|\mathcal{A}|}, \quad [\text{bit/sec/Hz/m}^2] \quad (3)$$

where  $Pr(x)$  is the probability of the UE being at a specific location  $x$  and  $\mathcal{X}$  is the set of locations included in the area  $\mathcal{A}$  satisfying  $Pr(x) > 0$  for all  $x \in \mathcal{X} \subset \mathcal{A}$ . For now, we assume the homogeneous user distribution such that the discrete set  $\mathcal{X}$  is a rectangular lattice with a small grid size and the probability of each location is the same, e.g.,  $Pr(x) = 1$  for all  $x \in \mathcal{X}$ . But we will discuss the inhomogeneous case at the end of Section III.

4) *Coverage*: Let us denote by  $\mathcal{A}_{i < j}$  the set of locations that have better SINR from BS  $i$  than  $j$ . We further denote by  $\mathcal{A}_{i = j}$  the set of boundaries having the same SINR from both BSs  $i$  and  $j$ . Then, the set of locations covered by BS  $k$  (or simply, coverage) can be written as<sup>2</sup>:

$$\mathcal{A}_k(\mathcal{B}) \doteq \{x | x \in \mathcal{A} \text{ s.t. } b(x, \mathcal{B}) = k\} = \bigcap_{b \in \mathcal{B}, b \neq k} \mathcal{A}_{k > b}. \quad (4)$$

<sup>1</sup>If there are more than one BSs providing the same highest signal strength, then any suitable tie-breaking rule is used, e.g., choosing the lower indexed BS.

<sup>2</sup>For simplicity, we ignore the boundaries in the definition of coverage.

## B. General Problem Statement

Consider an area of interest  $\mathcal{A}$  served by a wireless network operator whose access network consists of only macro BSs  $\mathcal{B}_M$ . We assume that the daily traffic profile<sup>3</sup> repeats periodically [17], [19], and that the required ASE  $S_{th}^t$  over time  $t$  corresponding to the traffic profile is already known. Suppose that the maximum required ASE  $S_{th}^{t^*}$  at the peak time  $t^* = \arg \max_t S_{th}^t$  during a day  $t \in [t_0, t_0+D)$  almost approaches to the one that can be provided by turning on all the macro BSs  $\mathcal{B}_M$ , i.e.,  $S(\mathcal{A}, \mathcal{B}_M) \simeq S_{th}^{t^*}$ . Thus, the operator wants to upgrade its access network by micro BSs which are considered as the cost-effective way of incrementally increasing capacity inside the initial macro cell deployment.

**General problem:** We want to minimize the total BS energy consumption during a day while providing  $\zeta \geq 1$  times higher ASE than before the upgrade. We can mathematically formulate this problem as the following optimization problem:

$$\begin{aligned} \text{(P)} \quad & \min_{\{\mathcal{B}^t\}} \int_{t_0}^{t_0+D} \left( P_M \cdot |\mathcal{B}_M^t| + P_m \cdot |\mathcal{B}_m^t| \right) dt \\ \text{s.t.} \quad & S(\mathcal{A}, \mathcal{B}^t) \geq \zeta \cdot S_{th}^t, \quad \forall t \in [t_0, t_0+D), \end{aligned} \quad (5)$$

where  $\mathcal{B}^t$  denotes the set of BSs that are turned on at time  $t$ ;  $P_M$  and  $P_m$  are operational power consumptions of macro and micro BSs, respectively.

**Problem separation:** The above general problem (P) can be separated into two subproblems: **(P1)** micro BSs deployment problem considering the peak time  $t^*$  and **(P2)** BSs operation problem during the off-peak period  $t \neq t^*$ .

It is desirable for the operator to minimize the cost for expanding its infrastructures while guaranteeing the required ASE. Therefore, The first problem is to find a minimal deployment of micro BSs which can support the peak time ASE. Note that this deployment issue is an offline problem that can be handled in a network coordinator. Once the micro BS deployment targeted at the peak time is done, the next problem is how to efficiently operate these micro BSs along with the existing macro BSs for energy conservation during the off-peak period. The solutions for the operation problem should be online distributed algorithms in order to be implemented in real systems. We will deal with these two problems one by one in the following consecutive sections.

## III. HCS DEPLOYMENT STRATEGY

First, we aim at finding a minimal deployment of micro BSs (i.e., minimizing the total power consumption) while satisfying the raised ASE requirement at the peak time,  $t = t^*$ :

$$\text{(P1)} \quad \min_{\mathcal{B}_m} |\mathcal{B}_m| \quad (6)$$

$$\text{s.t.} \quad S(\mathcal{A}, \mathcal{B}_M \cup \mathcal{B}_m) \geq \zeta \cdot S_{th}^{t^*} = \zeta \cdot S(\mathcal{A}, \mathcal{B}_M). \quad (7)$$

<sup>3</sup>The traffic profile for weekdays may differ from that for weekends.

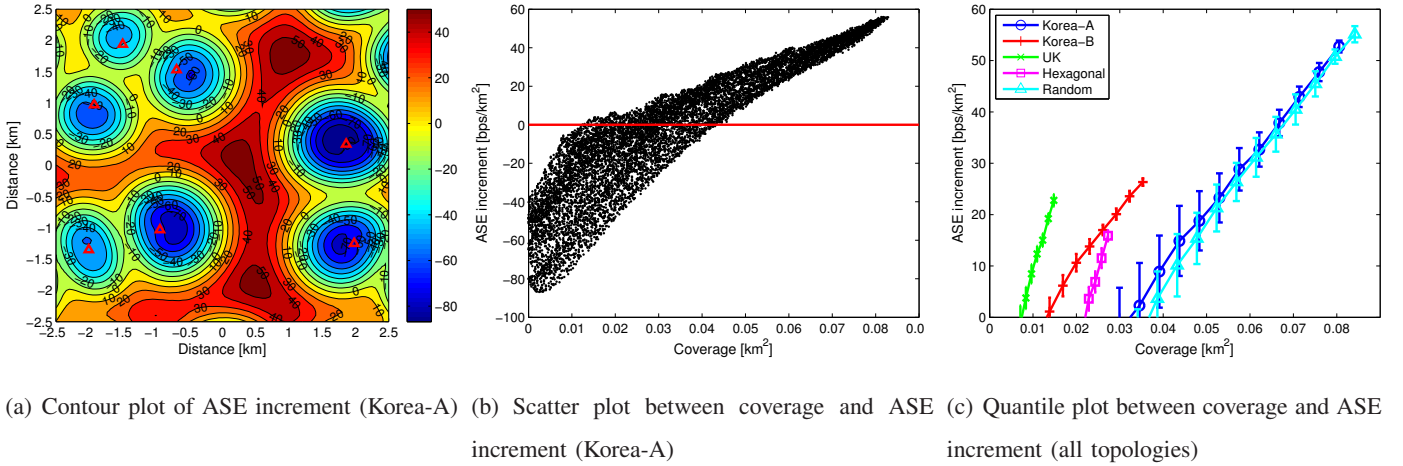


Fig. 1: Several interesting observations from various topologies including the real layout of macro BSs.

Note that **(P1)** can be also interpreted as a CAPEX minimization problem. The deployment problem **(P1)** is basically a combinatorial problem, and that makes it very difficult to find an optimal solution, especially, if the number of candidate locations is large. Therefore, in this paper, our goal is to develop a simple and efficient algorithm.

#### A. Key Observations

We shall start by presenting several observations from various topologies which help us to gain insight and develop an efficient algorithm. To obtain more realistic observations, we acquired the real macro BS topologies in the part of Korea [20] and Manchester, UK [3], [21] as well as typical hexagonal and random topologies. Listed here is brief information about the number of macro BSs and the size of observation area in the topologies that we used: (i) Korea-A: 7 BSs in  $5 \times 5 \text{ km}^2$ , (ii) Korea-B: 15 BSs in  $4.5 \times 4.5 \text{ km}^2$ , (iii) UK: 6 BSs in  $2.5 \times 2.5 \text{ km}^2$ , (iv) hexagonal: 7 BSs in  $4 \times 4 \text{ km}^2$ , and (v) random: 6 BSs in  $5 \times 5 \text{ km}^2$ . It is worth while mentioning that we ran simulations in much larger area than the above observation area to avoid edge effects.

We focus on the deployment of *one new micro BS* in the area that is covered by the existing set of macro BSs. The contour plot in Fig. 1(a) shows how much ASE a micro BS can improve according to the location of deployment. Although this is a snapshot from the topology of Korea-A, similar trends could be observed in the other topologies as well.

*Observation 1: As long as the new micro BS is placed not too close to the one of existing macro BSs, ASE can be expected to increase before the upgrade. Especially, the ASE increment becomes large as the distances from macro BSs increase.*

The wireless network operators are supposed to deploy a micro BS at the location where ASE can be improved. Therefore, throughout the paper, we only consider the set of candidate locations for the micro BS deployment as follows:

$$\forall k \in \mathcal{K}, \quad S(\mathcal{B} \cup \{k\}) > S(\mathcal{B}), \quad (8)$$

Now we examine how much area the micro BS can cover according to the location of deployment and investigate the correlation with ASE increment. In Fig. 1(b), ASE increment has a distinct tendency to increase with coverage. Interestingly, it becomes sharper as the coverage increases and this trend can be verified over the other topologies as well in the quantile plots in Fig. 1(c). This is desirable because we are interested in the locations that give high performance improvement. In such locations with small variance, we can almost surely assert that coverage and ASE increment have a near-monotonic relationship. Results from monotone test<sup>4</sup> (90.4~97.0% depending on the topologies) also support the following observation.

*Observation 2: The larger area can be covered by the new micro BS, the higher ASE increment is likely to be expected.*

Motivated by this observation, we assume that the following monotone relationship holds throughout the paper.

$$\begin{aligned} |\mathcal{A}_k(\mathcal{B} \cup \{k\})| &\geq |\mathcal{A}_{k'}(\mathcal{B}' \cup \{k'\})| \\ \Rightarrow S(\mathcal{B} \cup \{k\}) - S(\mathcal{B}) &\geq S(\mathcal{B}' \cup \{k'\}) - S(\mathcal{B}'), \end{aligned} \quad (9)$$

where  $k$  (or  $k'$ ) is the index of the micro BS.

These two observations are intuitively understandable. Consider the area covered by the micro BS far from existing macro BSs. Since the signals from the macro BSs are weak, the micro BS will provide the highest SINR to a large extent area. In addition to this large coverage, the area originally had low spectral efficiency, resulting in the high increment of ASE.

### B. Constant-Factor Approximation Greedy Algorithm

Prior to introducing a natural greedy algorithm for **(P1)**, we define a real-valued set function  $F : \mathcal{B}_m \rightarrow \mathbb{R}$  as follows:

$$F(\mathcal{B}_m) \doteq S(\mathcal{B}_M \cup \mathcal{B}_m) - S(\mathcal{B}_M), \quad (10)$$

which returns the ASE increment by additionally deploying the set of micro BSs  $\mathcal{B}_m$ .

---

#### Greedy deployment algorithm

---

- 1: Initialize  $\mathcal{B}_m^{\text{greedy}} = \emptyset$
  - 2: **do while**  $S(\mathcal{A}, \mathcal{B}_M \cup \mathcal{B}_m^{\text{greedy}}) < \zeta \cdot S_{th}^*$
  - 3:      $k^* = \arg \max_{k \in \mathcal{K}} F(\mathcal{B}_m^{\text{greedy}} \cup \{k\}) - F(\mathcal{B}_m^{\text{greedy}})$ ,
  - 4:      $\mathcal{B}_m \leftarrow \mathcal{B}_m \cup \{k\}$
  - 5: **end do**
- 

The greedy algorithm starts with the empty set  $\mathcal{B}_m^{\text{greedy}} = \emptyset$ , and iteratively adds the micro BS location having the highest increment among the set of candidate locations  $\mathcal{K}$  until ASE reaches a target value, i.e., satisfying the constraint (7).

<sup>4</sup>We randomly pick two points having positive ASE increments in Fig. 1(b) and check whether the slope between these points are positive or not.

*Theorem 3.1:* The ASE increment achieved by an optimal placement with the same number of micro BSs as the greedy algorithm cannot be more than a factor of  $e/(e-1)$  from the ASE increment achieved by the greedy algorithm.

$$\max_{|\mathcal{B}_m|=|\mathcal{B}_m^{\text{greedy}}|} F(\mathcal{B}_m) \leq \frac{e}{e-1} F(\mathcal{B}_m^{\text{greedy}}), \quad (11)$$

where the constant  $e$  is base of the natural logarithm.

*Proof:* In order to prove this theorem, we first need to show that the ASE increment function satisfies the following three properties: (i)  $F(\emptyset) = 0$ , (ii)  $F$  is increasing, and (iii)  $F$  is a submodular set function.  $F(\emptyset) = 0$  is trivial and  $F$  is an increasing function by the assumption (8). To prove the submodularity, it is enough to check that for all  $\mathcal{B}_m \subseteq \mathcal{B}_{m'} \subseteq \mathcal{K}$  and for an arbitrary chosen  $k \in \mathcal{K}/\mathcal{B}_{m'}$ , the following condition

$$F(\mathcal{B}_m \cup \{k\}) - F(\mathcal{B}_m) \geq F(\mathcal{B}_{m'} \cup \{k\}) - F(\mathcal{B}_{m'}) \quad (12)$$

holds. Since  $\mathcal{B}_m$  is the subset of  $\mathcal{B}_{m'}$  and  $F$  is increasing, we have the following two inequalities:

$$F(\mathcal{B}_m) \leq F(\mathcal{B}_{m'}) \quad \text{and} \quad (13)$$

$$\begin{aligned} |\mathcal{A}_k(\mathcal{B}_M \cup \mathcal{B}_m \cup \{k\})| &= \left| \bigcap_{b \in \mathcal{B}_M \cup \mathcal{B}_m} \mathcal{A}_{k>b} \right| \\ &\geq \left| \bigcap_{b \in \mathcal{B}_M \cup \mathcal{B}_{m'}} \mathcal{A}_{k>b} \right| \\ &= |\mathcal{A}_k(\mathcal{B}_M \cup \mathcal{B}_{m'} \cup \{k\})| \end{aligned} \quad (14)$$

By the assumption (9) and the definition of  $F$ , the coverage inequality (14) can be converted into the ASE inequality:

$$\begin{aligned} F(\mathcal{B}_m \cup \{k\}) &= S(\mathcal{B}_M \cup \mathcal{B}_m \cup \{k\}) - S(\mathcal{B}_M \cup \mathcal{B}_m) \\ &\geq S(\mathcal{B}_M \cup \mathcal{B}_{m'} \cup \{k\}) - S(\mathcal{B}_M \cup \mathcal{B}_{m'}) \\ &= F(\mathcal{B}_{m'} \cup \{k\}). \end{aligned} \quad (15)$$

Combining (13) and (15) completes the submodularity condition (12).

Nemhauser *et al.* studied a maximization problem for a nondecreasing submodular set function with  $F(\emptyset) = 0$ ,

$$\max_{\mathcal{Z}} F(\mathcal{Z}) \quad \text{s.t.} \quad |\mathcal{Z}| \leq K, \quad (16)$$

and they obtained that

$$\frac{\text{value of greedy approximation}}{\text{value of optimal solution}} \geq 1 - \left( \frac{K-1}{K} \right)^K. \quad (17)$$

Since our ASE increment function  $F(\cdot)$  is an increasing submodular function with  $F(\emptyset) = 0$ , the greedy algorithm is guaranteed to find a constant-factor approximation solution  $\mathcal{B}_m^{\text{greedy}}$ , such that

$$\begin{aligned} \frac{F(\mathcal{B}_m^{\text{greedy}})}{\max_{|\mathcal{B}_m|=|\mathcal{B}_m^{\text{greedy}}|} F(\mathcal{B}_m)} &\geq 1 - \left( \frac{|\mathcal{B}_m^{\text{greedy}}| - 1}{|\mathcal{B}_m^{\text{greedy}}|} \right)^{|\mathcal{B}_m^{\text{greedy}}|} \\ &\geq 1 - 1/e. \end{aligned}$$

This completes the proof. ■



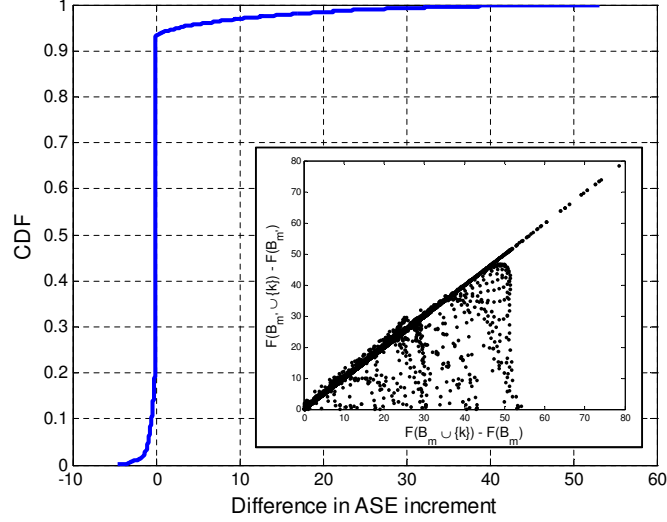


Fig. 2: Submodularity under the inhomogeneous environment.

*Remark 3.1:* In order to further reduce the computational complexity of the greedy algorithm, we may only check the locations near cell boundaries instead of all candidate locations. This is because the high ASE increment is likely to be obtained at cell boundaries based on Observation 1.

*Corollary 3.1:* So far we have assumed that micro BSs have the same operational power  $P_m$ . However, the above constant-factor approximation result can be extended to general cases [22], where each BS has a different operational power (say,  $P_k = P_i$  for  $k \in \mathcal{B}_i$ ). We only need to change the greedy algorithm as follows, i.e., finding the location with highest ASE increment per unit power consumption:

$$k^* = \arg \max_{k \in \mathcal{K}} \frac{F(\mathcal{B}_m^{\text{greedy}} \cup \{k\}) - F(\mathcal{B}_m^{\text{greedy}})}{P_k}. \quad (18)$$

*Remark 3.2:* Theorem 3.1 could be derived from the submodularity of ASE increment function under inhomogeneous traffic distributions. Although we could not prove the submodularity under inhomogeneous traffic distributions where  $Pr(x)$  is not the same over the area, we present some numerical results instead. For simulations, an inhomogeneous scenario having five randomly generated hot-spots ( $100 \times 100 \text{ m}^2$ ) in the Korea-A topology is considered. We investigate the probability that the submodularity condition  $F(\mathcal{B}_m \cup \{k\}) - F(\mathcal{B}_m) \geq F(\mathcal{B}_{m'} \cup \{k\}) - F(\mathcal{B}_{m'})$  for all  $\mathcal{B}_m \subseteq \mathcal{B}_{m'} \subseteq \mathcal{K}$  and for an arbitrary chosen  $k \in \mathcal{K}/\mathcal{B}_{m'}$  holds. Fig. 2 shows the CDF of the difference in ASE increment and the inner figure shows the scatter plot for details. We lose the submodularity because about 19% of locations violates the inequality. However, ASE decrements in such cases are relatively small and most of locations ( $> 80\%$ ) still satisfy the condition. Thus, we conjecture that the greedy deployment algorithm still works well under inhomogeneous traffic distributions.

#### IV. HCS OPERATION STRATEGY

Since BSs are deployed to support the peak time traffic, they will be under-utilized most of off-peak times,  $t \neq t^*$ . If an appropriate dynamic BS operation algorithm is not employed, then a considerable amount of energy will be wasted. Thus, our objective at the off-peak period is to find a dynamic operation of BSs that minimizes the total operational power consumption while satisfying the raised ASE requirement<sup>5</sup>:

$$\begin{aligned} \text{(P2)} \quad & \min_{\mathcal{B}^t} P_M \cdot |\mathcal{B}_M^t| + P_m \cdot |\mathcal{B}_m^t| \\ \text{s.t.} \quad & S(\mathcal{A}, \mathcal{B}^t) \geq \zeta \cdot S_{th}^t. \end{aligned} \quad (19)$$

The operation problem **(P2)** is a combinatorial optimization problem as well. Thus, in the following consecutive subsection, we propose a suboptimal offline centralized algorithm and two online distributed BS switching algorithms.

##### A. Centralized BS Switching Algorithm

Since there is a similarity between the deployment and operation problems, we may use the generalized deployment algorithm in (18) as a centralized algorithm for the operation problem as follows:

$$k^* = \arg \max_{k \in \mathcal{B}} \frac{F(B^t \cup \{k\}) - F(B^t)}{P_k}. \quad (20)$$

This centralized switching algorithm has a nice feature of the constant-factor approximation; however, the algorithm not only requires many feedbacks from all BSs to the network coordinator but also should be started from the empty set (i.e., turning off all BSs), which makes it difficult for the centralized algorithm to be implemented in practice. In order to overcome such difficulties, we propose simple and distributed online algorithms in the next subsection.

##### B. Distributed BS Switching Algorithm

Using the Lagrangian relaxation with a multiplier  $\lambda$ , the BS operation problem **(P2)** can be separated by the summation of the switching problem at each BS as follows.

$$\begin{aligned} L(\mathcal{B}^t, \lambda) &= \sum_{b \in \mathcal{B}^t} P_b + \lambda [\zeta \cdot S_{th}^t - S(\mathcal{A}, \mathcal{B}^t)] \\ &= \sum_{b \in \mathcal{B}^t} \left[ P_b a^t(b) + \frac{\lambda}{|\mathcal{A}|} \left( \frac{\zeta \cdot |\mathcal{A}|}{|\mathcal{B}|} S_{th}^t - \sum_{x \in \mathcal{X}_b} C(x, \mathcal{B}^t) \right) \right] \\ &= \sum_{b \in \mathcal{B}^t} L_b(a^t(b), \lambda), \end{aligned}$$

where  $a^t(b)$  denotes the indicator of BS status, i.e.,  $a^t(b) = 1$  when the BS  $b$  is on at time  $t$ , and 0 otherwise;  $\mathcal{X}_b$  denotes the set of locations included in the serving area of BS  $b$ , and

$$L_b(a^t(b), \lambda)$$

<sup>5</sup>Note that since the traffic profiles are usually to remain stationary at timescales beyond an hour [19], the original problem **(P)** only needs to be solved at several discrete times.

$$= \begin{cases} \frac{\lambda}{|\mathcal{A}|} \left( \frac{\zeta \cdot |\mathcal{A}|}{|\mathcal{B}|} S_{th}^t - \sum_{x \in \mathcal{X}_b} C(x, \mathcal{B}^t - \{b\}) \right), & \text{if } a^t(b) = 0, \\ \frac{\lambda}{|\mathcal{A}|} \left( \frac{\zeta \cdot |\mathcal{A}|}{|\mathcal{B}|} S_{th}^t - \sum_{x \in \mathcal{X}_b} C(x, \mathcal{B}^t) \right) + P_b, & \text{if } a^t(b) = 1. \end{cases} \quad (21a)$$

$$= \begin{cases} \frac{\lambda}{|\mathcal{A}|} \left( \frac{\zeta \cdot |\mathcal{A}|}{|\mathcal{B}|} S_{th}^t - \sum_{x \in \mathcal{X}_b} C(x, \mathcal{B}^t) \right) + P_b, & \text{if } a^t(b) = 1. \end{cases} \quad (21b)$$

To minimize the relaxation gap, the network coordinator updates the Lagrangian multiplier using gradient descent iterative method with a small step size  $\epsilon > 0$ , i.e.,

$$\lambda \leftarrow \lambda + \epsilon \left[ \zeta \cdot S_{th}^t - S(\mathcal{A}, \mathcal{B}^t) \right], \quad (22)$$

where  $S(\mathcal{A}, \mathcal{B}^t)$  can be calculated by collecting local ASE in each BS as follows:

$$S(\mathcal{A}, \mathcal{B}^t) = \frac{1}{|\mathcal{A}|} \sum_{b \in \mathcal{B}^t} |\mathcal{A}_b| \cdot S(\mathcal{A}_b, \mathcal{B}^t). \quad (23)$$

For any given  $\lambda$ , the BS  $b$  needs to be turned off for energy saving if the difference between (21a) and (21b) is less than or equal to zero, i.e.,

$$\begin{aligned} L_b(0, \lambda) - L_b(1, \lambda) &\leq 0 \\ \Leftrightarrow \frac{|\mathcal{A}_b| \cdot \{S(\mathcal{A}_b, \mathcal{B}^t) - S(\mathcal{A}_b, \mathcal{B}^t - \{b\})\}}{P_b} &\leq \frac{|\mathcal{A}|}{\lambda}. \end{aligned} \quad (24)$$

This condition (24) can be interpreted as follows: (i) The less difference in spectral efficiency (i.e., small impact on QoS) the BS has and/or (ii) the larger operational power (i.e., large energy saving) the BS consumes, the more likely the BS is switched off.

With help of the switching off condition, we propose a BS switching algorithm (**S-OFF1**) in the following. Please see Fig. 3 for a pictorial description.

---

#### **(S-OFF1) SINR-based distributed switching algorithm**

---

At each time  $t$ , each BS  $b$  reports current local information  $|\mathcal{A}_b| \cdot S(\mathcal{A}_b, \mathcal{B}^t)$  to the network coordinator, and receives the Lagrangian multiplier  $\lambda$ . If the performance decrement in spectral efficiency per unit operational power is less than a certain threshold, then the BS  $b$  will be switched off.

$$\frac{|\mathcal{A}_b| \cdot \{S(\mathcal{A}_b, \mathcal{B}^t) - S(\mathcal{A}_b, \mathcal{B}^t - \{b\})\}}{P_b} \leq \frac{|\mathcal{A}|}{\lambda}. \quad (25)$$

The BS switching-on procedure can be accomplished by the reverse way of the switching-off procedure. Without any additional calculation in off-state, the BS  $b$  is switched on when the target ASE reaches the same value that the BS was originally switched off.

In (**S-OFF1**), each BS requires SINR estimations before and after turning-off from UEs in its coverage. To reduce the signal processing overhead of UEs, we propose (**S-OFF2**) based on SNR estimations.

---

#### **(S-OFF2) SNR-based distributed switching algorithm**

---

$$\frac{|\mathcal{A}_b| \cdot \{S_{\sigma^2}(\mathcal{A}_b, \mathcal{B}^t) - S_{\sigma^2}(\mathcal{A}_b, \mathcal{B}^t - \{b\})\}}{P_b} \leq \frac{|\mathcal{A}|}{\lambda}. \quad (26)$$

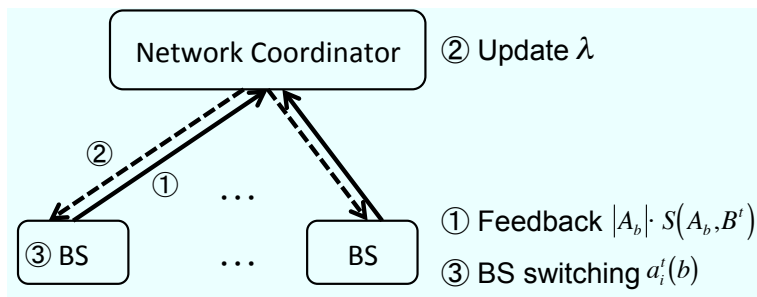


Fig. 3: Flow of distributed BS switching algorithm

where  $S_{\sigma^2}(\mathcal{A}, \mathcal{B}) = \frac{1}{|\mathcal{A}|} \sum_{x \in \mathcal{X}} \log_2(1 + E_{b(x, \mathcal{B})}(x)/\sigma^2)$ .

*Lemma 4.1:* The ASE differences of SINR-based and SNR-based distributed algorithms satisfy the following:

$$S(\mathcal{A}_b, \mathcal{B}^t) - S(\mathcal{A}_b, \mathcal{B}^t - \{b\}) \leq S_{\sigma^2}(\mathcal{A}_b, \mathcal{B}^t) - S_{\sigma^2}. \quad (27)$$

Accordingly, **(S-OFF1)** turns off more BSs than **(S-OFF2)**, resulting in more energy saving.

*Proof:* Denote the indexes of BSs that offers the best and the second best signal strength by  $k_1 = b(x, \mathcal{B}^t)$  and  $k_2 = b(x, \mathcal{B}^t - \{k_1\})$ , respectively. The difference in spectral efficiency based on SINR at location  $x$  can be expressed as

$$\begin{aligned} & C(x, \mathcal{B}^t) - C(x, \mathcal{B}^t - \{b\}) \\ &= \log_2 \left\{ 1 + \frac{E_{k_1}(x)}{E_{k_2}(x) + I_x + \sigma^2} \right\} - \log_2 \left\{ 1 + \frac{E_{k_2}(x)}{I_x + \sigma^2} \right\} \\ &\leq \log_2 \left\{ 1 + \frac{E_{k_1}(x)}{I_x + \sigma^2} \right\} - \log_2 \left\{ 1 + \frac{E_{k_2}(x)}{I_x + \sigma^2} \right\} \\ &= \log_2 \left\{ \frac{I_x + \sigma^2 + E_{k_1}(x)}{I_x + \sigma^2 + E_{k_2}(x)} \right\} \\ &\leq \log_2 \left\{ \frac{\sigma^2 + E_{k_1}(x)}{\sigma^2 + E_{k_2}(x)} \right\} \\ &= C_{\sigma^2}(x, \mathcal{B}^t) - C_{\sigma^2}(x, \mathcal{B}^t - \{b\}) \end{aligned} \quad (28)$$

where  $I_x = I(x, \mathcal{B} - \{k_1\})$ . Note that the last inequality holds because  $\log_2 \left( \frac{z + E_{k_1}(x)}{z + E_{k_2}(x)} \right)$  is a monotone decreasing convex function of  $z$  when  $E_{k_1}(x) > E_{k_2}(x)$  [23]. By the definition of ASE and (28), we can have the condition (27). ■

## V. NUMERICAL RESULTS

We consider the deployment of macro BSs as shown in Fig. 4 for our simulation. There are 10 macro BSs in  $8 \times 8 \text{ km}^2$ . In order to avoid edge effects, we only observe the area of  $5 \times 5 \text{ km}^2$ . Typical transmission and total operational powers for macro and micro BSs are summarized in Table I [24], [25]. In modeling the propagation environment, the modified COST 231 Hata path loss model with macro BS height  $h = 32 \text{ m}$  and micro BS height

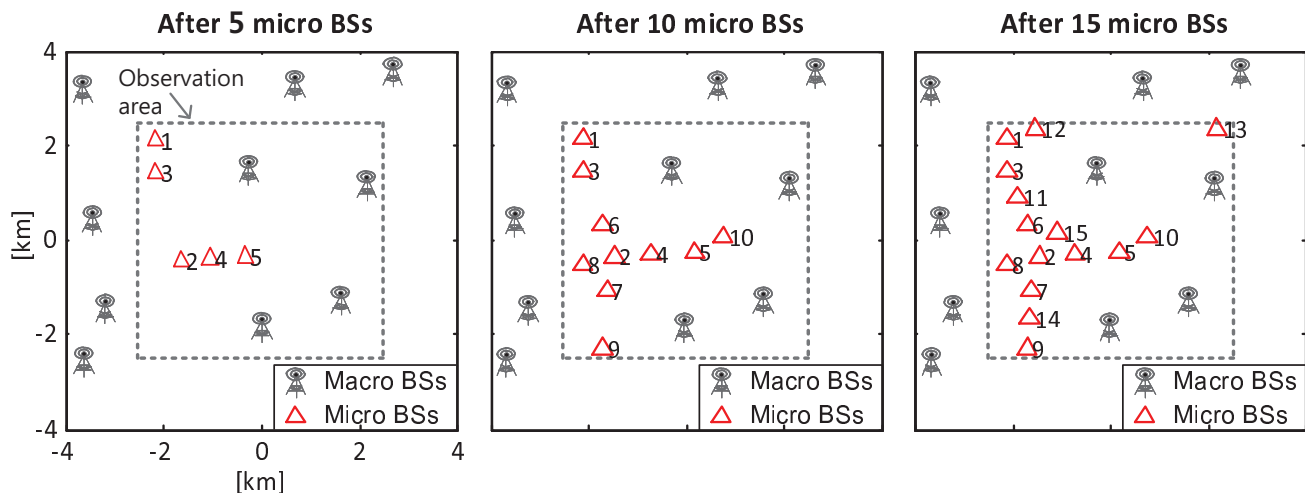


Fig. 4: Snapshot of BS deployment (Micro 2W).

TABLE I: Typical BS energy consumption.

Macro BS	$p_M$	10W	20W	40W
	$P_M$	638W	865W	1317W
Micro BS	$p_m$	500mW	1W	2W
	$P_m$	35W	38W	43W

$h = 12.5$  is used. The other parameters for the simulations follow the suggestions in the IEEE 802.16m evaluation methodology document [26].

#### A. Base Station Deployment

On top of the deployment of macro BSs, we consider the deployment of micro BSs to further increase ASE in the area of interest. The proposed greedy deployment algorithm in Section III shown to be a constant-factor approximation of optimal deployment is evaluated. Fig. 4 show the snapshots of the greedy algorithm after 5 and 10 micro BSs additionally deployed. As expected, the micro BSs tend to be placed in the boundaries of the cell because this makes each micro BS cover larger area, resulting in more ASE increment.

In Fig. 5, we investigate the performance improvement according to the additional deployment of BSs having different transmission powers. Four types of BSs are considered: the macro BS with transmit power of 20W and the micro BSs with transmit power of 0.5W, 1W and 2W, respectively. There are diminishing returns on the normalized ASE increment. This is not only because the coverage of newly deployed BS will shrink but the amount of interference in the network increase as the number of BSs increases.

To meet the target ASE increment of 10%, while only five additional macro BSs are needed, 15, 22 or 30 micro BSs (three to six times more than macro BSs) are needed depending on their transmission powers. Nevertheless,

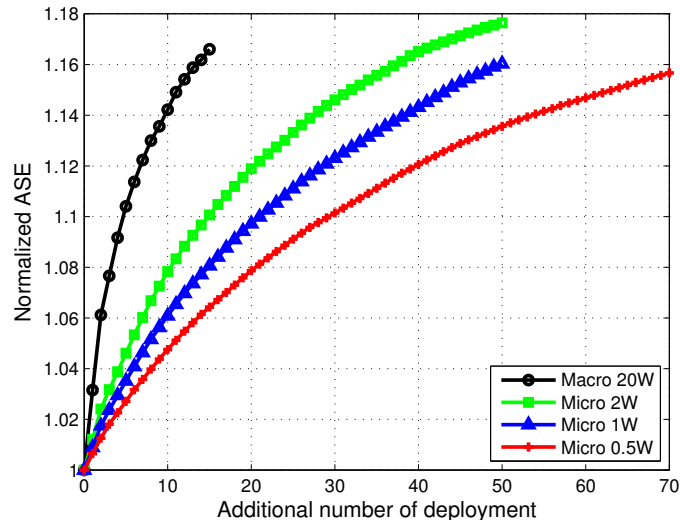


Fig. 5: Normalized ASE increment according to the deployment of different types of BSs.

TABLE II: Additional total power consumption required for the target ASE increment.

		Macro	Micro	Micro	Micro
		20W	2W	1W	0.5W
Target ASE	10%	4325W	645W	836W	1050W
increment	15%	9515W	1476W	1672W	2240W

the transmission power consumptions ( $p_M$  and  $p_m$ ) of additional micro BSs are much less than that of additional macro BSs. For example, while 100W is consumed by the macro BSs, only 30W, 22W, or 15W is consumed by the micro BSs.

When we reflect the total power consumptions ( $P_M$  and  $P_m$ ) in Table I, the advantage of micro BSs becomes more clear. Table II shows the required the additional total power consumptions for different target ASE increment. Compared to the case of macro BSs, deploying micro BSs can reduce more than 3kW and 6kW for the target ASE increment 10% and 15%, respectively. This corresponds to almost 75-80% savings in the total power consumptions.

### B. Base Station Operation

We now examine the performance of the proposed BS switching algorithms in Section IV. Fig. 6 shows the percentage of additional power consumption for different algorithms by varying the normalized required ASE  $S_{th}^t/S_{th}^{t*}$  compared to the result of an optimal exhaustive search. First of all, it is worthwhile mentioning that such simple distributed algorithms can closely approximate the complex centralized algorithm. When the normalized required ASE is less than 0.4, the centralized and two distributed algorithms consume the same amount of energy with the optimal solution. However, as the normalized required ASE increases over 0.4, performance gaps begin

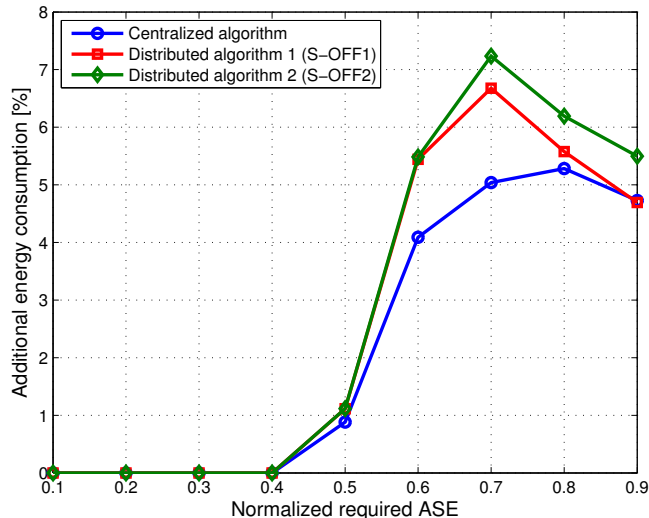


Fig. 6: Percentage of additional energy consumption compared to that of an optimal exhaustive search.

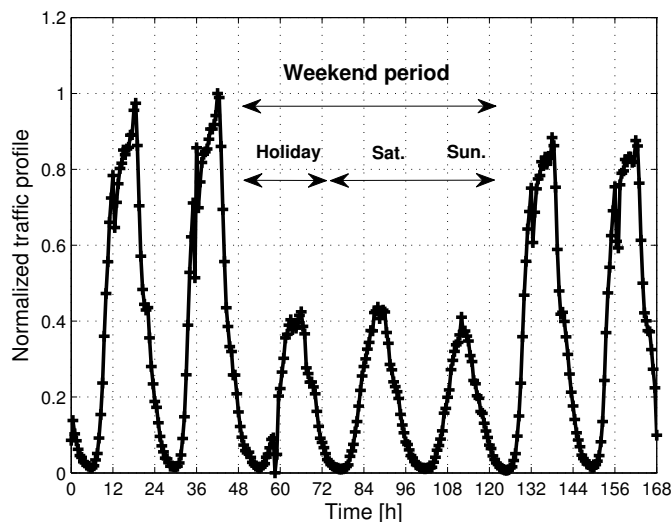


Fig. 7: Normalized traffic profile during one week from a real cellular data trace.

to arise. For example, additional 5.0%, 6.7% and 7.2% energies are used (at  $S_{th}^t/S_{th}^{t^*} = 0.7$ ) in the centralized and two distributed algorithms, respectively.

To obtain more realistic results, we further consider traffic profiles in a metropolitan urban area during one week as shown in Fig. 7 that is recorded by an anonymous wireless network operator. The low traffic period (less than 0.4 of the maximum value) is about 65% of time assuming two weekend days in a typical week. This implies that our distributed algorithms can obtain the same performance as the optimal solution during 65% of time and can still be within about 7% from the optimal solution during the rest of time.

Fig. 8 illustrates the energy consumption ratio during one day compared to the case without the dynamic BS

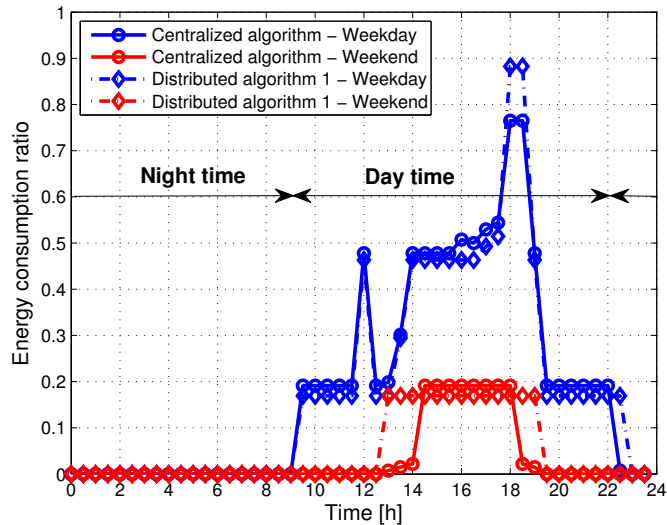


Fig. 8: Energy consumption ratio during one day (macro 20W & micro 1W).

TABLE III: Energy saving ratio during one day (macro 20W & the target ASE increment of 15%).

		Micro 2W	Micro 1W	Micro 0.5W
Weekday	Cent.	81.1%	80.9%	82.9%
	S-OFF1	80.9%	80.6%	82.0%
	S-OFF2	79.6%	80.5%	81.6%
Weekend	Cent.	96.7%	96.6%	97.2%
	S-OFF1	95.3%	95.4%	96.1%
	S-OFF2	95.3%	95.3%	96.1%

operation. It is shown that most of BSs can be turned off at night time, and the energy consumption is reduced by less than half during most of day time. Note that we used the BS topology for this simulation which is obtained from the proposed deployment algorithm in the previous subsection V-A. Table III summarizes the total energy saving ratio for different algorithms during weekday and weekend. It is expected that 80% and 95% of energy consumption can be saved during weekday and weekend, respectively. Given that OPEX of wireless network operators for electricity is more than 10 billion dollars globally [3], this could translate to huge economic benefit to the operators.

## VI. CONCLUSION

Hierarchical cell structure, consisting of cells with different sizes and ranging from macro to micro cells, will play a pivotal role in next-generation wireless networks. It can increase not only spectral efficiency but also cost-effectiveness and power-efficiency. In this paper, we proposed an energy-aware hierarchical cell configuration



framework that has theoretical results as well as practical guidelines on how wireless network operators manage their BSs. We specifically focused on a problem pertaining to total energy consumption minimization while satisfying the requirement of ASE, and decomposed it into deployment problem at peak time and operation problem at off-peak time. For the deployment problem, we proposed a constant-factor approximation greedy algorithm. Since there is a similarity between the deployment and operation problems, the greedy algorithm can be applied as a centralized offline solution for the operation problem. We further propose two distributed online switching algorithms using Lagrangian relaxation to have more practical solutions. Extensive simulations based on the acquired real BS topologies and traffic profiles show that the proposed deployment and operation algorithms can dramatically save the total energy consumption.

## REFERENCES

- [1] X. Wu, B. Murherjee, and D. Ghosal, "Hierarchical architectures in the third-generation cellular network," *IEEE Wireless Commun. Mag.*, vol. 11, no. 3, pp. 62–71, June 2004.
- [2] H. Claussen, L. T. W. Ho, and L. G. Samuel, "Financial analysis of a pico-cellular home network deployment," in *Proc. of IEEE ICC*, Glasgow, Scotland, June 2007, pp. 5604–5609.
- [3] E. Oh, B. Krishnamachari, X. Liu, and Z. Niu, "Towards dynamic energy-efficient operation of cellular network infrastructure," *IEEE Commun. Mag.*, Nov. 2010.
- [4] M. A. Marsan, L. Chiaraviglio, D. Ciullo, and M. Meo, "Optimal energy savings in cellular access networks," in *Proc. of IEEE GreenComm*, Dresden, Germany, June 2009.
- [5] E. Oh and B. Krishnamachari, "Energy savings through dynamic base station switching in cellular wireless access networks," in *Proc. of IEEE Globecom*, Miami, FL, Dec. 2010.
- [6] C. S. Kang, H. S. Cho, and D. K. Sung, "Capacity analysis of spectrally overlaid macro/microcellular CDMA systems supporting multiple types of traffic," *IEEE Trans. Veh. Technol.*, vol. 52, no. 2, pp. 333–346, Mar. 2003.
- [7] V. Chandrasekhar and J. G. Andrews, "Spectrum allocation in tiered cellular networks," *IEEE Trans. Commun.*, vol. 57, no. 10, pp. 3059–3068, Oct. 2009.
- [8] D. López-Pérez, A. Valcarce, G. De La Roche, and J. Zhang, "OFDMA femtocells: A roadmap on interference avoidance," *IEEE Commun. Mag.*, vol. 47, no. 9, pp. 41–48, Sept. 2009.
- [9] S. H. Shin and K. S. Kwak, "Power control for CDMA macro-micro cellular system," in *Proc. of IEEE VTC*, Boston, MA, Sept. 2000.
- [10] S. Kishore, L. J. Greenstein, H. V. Poor, and S. C. Schwartz, "Uplink user capacity in a CDMA system with hotspot microcells: effects of finite transmit power and dispersion," *IEEE Trans. Wireless Commun.*, vol. 5, no. 2, pp. 417–426, Feb. 2006.
- [11] S. Kim, D. Hong, and J. Cho, "Hierarchical cell deployment for high speed data CDMA systems," in *Proc. of IEEE WCNC*, Orlando, FL, Mar. 2002.
- [12] H. Claussen, "Co-channel operation of macro- and femtocells in a hierarchical cell structure," *Int. J. Wireless Inf. Networks*, vol. 15, no. 3, pp. 137–147, Dec. 2008.
- [13] D. Stamatelos and A. Ephremides, "Spectral efficiency and optimal base placement for indoor wireless networks," *IEEE J. Select. Areas Commun.*, vol. 14, no. 4, pp. 651–661, 1996.
- [14] A. Srinivas and E. Modiano, "Joint node placement and assignment for throughput optimization in mobile backbone networks," in *Proc. IEEE INFOCOM*, Phoenix, AZ, Apr. 2008.
- [15] S. Zhou, J. Gong, Z. Yang, Z. Niu, and P. Yang, "Green mobile access network with dynamic base station energy saving," in *Proc. of ACM MobiCom*, Beijing, China, Sept. 2009.

- [16] L. Chiaraviglio, D. Ciullo, M. Meo, M. A. Marsan, and I. Torino, "Energy-aware UMTS access networks," in *Proc. of WPMC Symposium*, Lapland, Finland, Sept. 2008.
- [17] M. A. Marsan and M. Meo, "Energy efficient management of two cellular access networks," in *Proc. of ACM GreenMetrics*, Seattle, WA, June 2009.
- [18] M. S. Alouini and A. J. Goldsmith, "Area spectral efficiency of cellular mobile radio systems," *IEEE Trans. Veh. Technol.*, vol. 48, no. 4, pp. 1047–1066, July 1999.
- [19] D. Willkomm, S. Machiraju, J. Bolot, and A. Wolisz, "Primary users in cellular networks: A large-scale measurement study," in *Proc. of IEEE DySPAN*, Chicago, IL, Oct. 2008.
- [20] K. Son, S. Lee, Y. Yi, and S. Chong, "Practical dynamic interference management in multi-carrier multi-cell wireless networks: A reference user based approach," in *Proc. WiOpt*, Avignon, France, June 2009.
- [21] "Sitefinder: Mobile phone base station database," Ofcom. [Online]. Available: <http://www.sitefinder.ofcom.org.uk/>.
- [22] M. Sviridenko, "A note on maximizing a submodular set function subject to knapsack constraint," *Operations Research Letters*, vol. 32, pp. 41–43, 2004.
- [23] S. Boyd and L. Vandenberghe, *Convex Optimization*. Cambridge University Press, 2004.
- [24] A. J. Fehske, F. Richter, and G. P. Fettweis, "Energy efficiency improvements through micro sites in cellular mobile radio networks," in *Proc. of IEEE GreenComm*, Honolulu, HI, Dec. 2009.
- [25] O. Arnold, F. Richter, G. Fettweis, and O. Blume, "Power consumption modeling of different base station types in heterogeneous cellular networks," in *Proc. of ICT MobileSummit*, Florence, Italy, June 2010.
- [26] *IEEE 802.16m-08/004r5: IEEE 802.16m Evaluation Methodology Document (EMD)*, IEEE Std. 802.16m, 2009.